

# Ultrasound-Modulated Bubble Propulsion of Chemically-Powered Microengines

Tailin Xu<sup>1,2,‡</sup>, Fernando Soto<sup>1,‡</sup>, Wei Gao<sup>1</sup>, Victor Garcia-Gradilla<sup>1</sup>, Jinxing Li<sup>1</sup>, Xueji Zhang<sup>2</sup>, Joseph Wang<sup>1\*</sup>

<sup>1</sup>Department of Nanoengineering, University of California-San Diego, La Jolla, California, 92093, USA

<sup>2</sup>Research Center for Bioengineering and Sensing Technology, University of Science and Technology Beijing, Beijing 100083, P. R. China

<sup>‡</sup>These authors contributed equally to this work

Address correspondence to [josephwang@ucsd.edu](mailto:josephwang@ucsd.edu).

## Supporting Videos

Video S1. Bubble evolution and ejection behavior of the ‘braking’ mechanism of the chemically-powered microengines.

Video S2. Ultrasound triggered ‘stop and go’ of a micromotor.

Video S3. Speed modulation of a microengine by tailoring the ultrasound power.

Video S4. The influence of ultrasound on a superfast moving micromotor.

## Supporting Figures

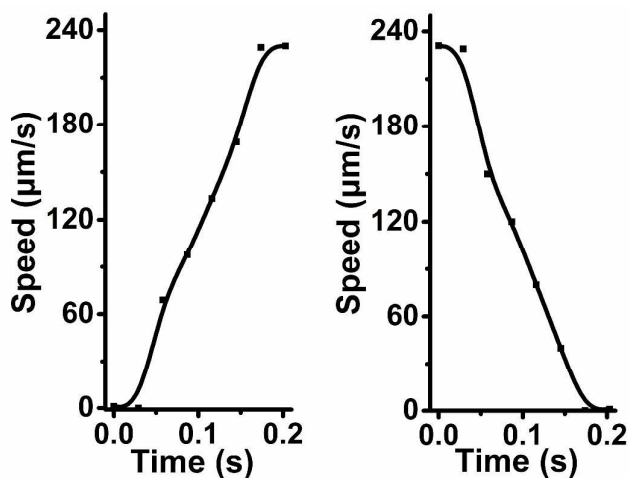


Fig. S1. Speed response of the microengines after applying (Left) and stopping (Right) the ultrasound field (10 V, 1 MHz).

## Experimental Section

### Reagents and Apparatus

Cyclopore polycarbonate membranes, with 5 μm diameter conical-shaped micropores, were purchased from Whatman (Catalog No 7060-2511; Maidstone, U.K.). The Pt–Ni mixture solution was prepared by mixing the same volume of a commercial platinum solution (Platinum RTP; Technic Inc, Anaheim, CA) and a nickel solution (containing a mixture of 20 g/L NiCl<sub>2</sub>•6H<sub>2</sub>O, 515 g/L Ni(H<sub>2</sub>NSO<sub>3</sub>)<sub>2</sub>•4H<sub>2</sub>O, and 20 g/L H<sub>3</sub>BO<sub>3</sub>). 3, 4-ethylenedioxythiophene (EDOT), sodium dodecyl sulfate (SDS, MW 288.38 g/mol), potassium nitrate, hydrogen peroxide and sodium cholate (NaCh) were all purchased from Sigma. All chemicals were analytical-grade reagents and were used as received without any further purification. The corresponding solutions were prepared by dilution in 18.2 MΩ·cm Milli-Q deionized water when not otherwise specified. Experiments were carried out at room temperature. All controlled-potential experiments were performed with a CHI 660D potentiostat (CH Instruments, Austin, TX). A Nikon Eclipse 80i microscope, coupled with a 10x objective, a Photometrics CoolSnap HQ2 CCD camera, and a MetaMorph 7.6 software (Molecular Devices, Sunnyvale, CA) were used for capturing movies at a frame rate of 10 frames per sec.

### Synthesis of micromotors

Self-propelled catalytic microengines were prepared by a template-directed electrodeposition method using polycarbonate membranes, with conical-shaped micropores.<sup>1</sup> The outer poly (3,4-ethylenedioxythiophene) (PEDOT) layer was prepared by electropolymerization at +0.80 V using a charge of 0.3 C from a plating solution containing 10 mM EDOT, 7.5 mM potassium nitrate and 100 mM SDS. Subsequently, an intermediate Ni layer (essential for magnetic guidance) was deposited potentiostatically at -1.2 V for 3.8 C from the Ni-Pt plating mixture. Finally, the inner catalytic Pt layer was deposited galvanostatically at -2 mA for 1300 s. Other types of spherical motors tested for the new speed modulation capability were Al-based micromotors<sup>2</sup> and silver based micromotors.<sup>3</sup>

#### Ultrasound equipment

The ultrasonic experiments were carried out in a cell similar to that described previously.<sup>4,5</sup> The cell was made in a covered glass slide (75 x 25 x 1 mm). The piezoelectric transducer which produces the ultrasound waves (Physik Instrumente PZT ring 0.5 mm thickness, 10 mm outside diameter by 5mm center hole diameter) was attached to the bottom center of the glass slide. The continuous ultrasound sine wave was applied via a piezoelectric transducer, through an Agilent 15MHz arbitrary waveform generator, in connection to a home-made power amplifier. The applied continuous sine waveform had a frequency of 1.00 MHz and a voltage amplitude, varied between 0 and 10.0 V, as needed for controlling the intensity of the ultrasonic wave. The electric signal was monitored using a 20 MHz Tektronix 434 storage oscilloscope.

#### **Mathematic Discussions on Bjerknes forces**

The interference between different standing acoustic waves establishes a differential pressure field in the fluid; acoustic radiation forces drive gas bubbles to nodes or antinodes in the acoustic pressure field. The acoustic radiation forces on gas bubbles are normally referred to as Bjerknes forces.<sup>6</sup> The Bjerknes forces are used to describe the instantaneous forces exerted on the bubbles by the surrounding (acoustically excited) liquid. The Bjerknes forces are normally divided into two basic types: primary Bjerknes forces and secondary Bjerknes forces. The primary Bjerknes forces are experienced by single bubbles which cause bubbles to migrate in an acoustic field or to gather in certain areas, such as pressure nodes. The secondary Bjerknes forces are responsible for bubble interactions which make bubbles attract each other.<sup>6</sup>

Bubble is assumed to be a sphere surrounded by an ideal (non-viscous and non-heat-conducting liquid) with a radius of  $R_0$  (4 -10  $\mu\text{m}$ ). It is much smaller as

compared to the wavelength of sound  $\lambda$  (1.5 mm, calculated as  $\lambda=c/f$  where the  $c$  is the speed of sound in water (1496 m/s) and  $f$  is the frequency of applied ultrasound field (1.0 MHz)). Considering these points, the primary Bjerknes force ( $F_1$ ) can be expressed as:<sup>7</sup>

$$F_1 = \frac{2\pi|A_m|^2 \delta R_0 \kappa}{\rho_0 \omega^2 \left[ \left(1 - \omega_0^2 / \omega^2\right)^2 + \delta^2 \right]} \quad (1)$$

$$\omega_0 = \frac{1}{R_0} \left[ \frac{3\gamma}{\rho_0} \left( P_0 + \frac{2\sigma}{R_0} \right) - \frac{2\sigma}{\rho_0 R_0} \right]^{1/2} \quad (2)$$

where  $\rho_0$  is the equilibrium liquid density,  $\omega_0$  is the resonance angular frequency of the bubble (calculated by equation 2),  $P_0$  is the hydrostatic pressure in the liquid,  $\sigma$  is the surface tension,  $\gamma$  is the ratio of specific heats of the gas in the bubble,  $\omega$  is the driving acoustic angular frequency (1.0 MHz),  $\delta$  is the total damping constant,  $A_m$  is the complex pressure amplitude which is proportional to applied transducer potential and  $\kappa$  is the wave vector in the liquid. Under our current experimental setting, we obtain that:

$$F_1 \propto |A_m|^2 \quad (3)$$

In addition, the secondary Bjerknes force ( $F_2$ ) can be expressed as:<sup>5</sup>

$$F_2 = \frac{2\pi R_{10} R_{20} |A_m|^2 \left[ \left(1 - \omega_1^2 / \omega^2\right) \left(1 - \omega_2^2 / \omega^2\right) + \delta_1 \delta_2 \right]}{\rho_0 \omega^2 L^2 \left[ \left(1 - \omega_1^2 / \omega^2\right)^2 + \delta_1^2 \right] \left[ \left(1 - \omega_2^2 / \omega^2\right)^2 + \delta_2^2 \right]} \quad (4)$$

where  $R_{10}$  and  $R_{20}$  are the equilibrium radius which is dependent on the size of the microengines ( $R_{10}=R_{20}$  for the same engine),  $\omega_1$  and  $\omega_2$  are resonance angular frequencies of the bubbles,  $\delta_1$  and  $\delta_2$  are their total damping constants, and  $L$  is the distance between two bubbles. Considering  $\omega_1=\omega_2$  and  $\delta_1=\delta_2$  for bubbles generated from the same engine,  $F_2$  is always  $>0$  (the bubbles attract together) and we obtain that:

$$F_2 \propto |A_m|^2 / L^2 \quad (5)$$

From equations 3 and 5, we find that applied transducer potentials have a direct influence on the resulting Bjerknes forces. When the applied potential is increasing, the primary Bjerknes forces and the secondary Bjerknes forces also become larger. Higher US power thus leads to higher Bjerknes forces and thus a faster bubble immigration and aggregation process, which leads to further deceleration on the speed of microengines.

## References

- (1) Gao, W.; Sattayasamitsathit, S.; Orozco, J.; Wang, J. *J. Am. Chem. Soc.* **2011**, *133*, 11862.
- (2) Gao, W.; D'Agostino, M.; Garcia-Gradilla, V.; Orozco, J.; Wang, J. *Small* **2013**, *9*, 467.
- (3) Wang, H.; Zhao, G.; Pumera, M. *J. Am. Chem. Soc.* **2014**, *136*, 2719.
- (4) Garcia-Gradilla, V.; Orozco, J.; Sattayasamitsathit, S.; Soto, F.; Kuralay, F.; Pourazary, A.; Katzenberg, A.; Gao, W.; Shen, Y.; Wang, J. *ACS Nano* **2013**, *7*, 9232.
- (5) Wang, W.; Castro, L. A.; Hoyos, M.; Mallouk, T. E. *ACS Nano* **2012**, *6*, 6122.
- (6) Woodside, S. M.; Bowen, B. D.; Piret, J. M. *Aiche J.* **1997**, *43*, 1727.
- (7) Doinikov, A. A. *Bubble and Particle Dynamics in Acoustic Fields: Modern Trends and Applications*; Research Signpost, Kerala, 2005.